# Streamflow timing of mountain rivers in spain: recent changes and future projections

Moran, Enrique; Lorenzo-Lacruz, Jorge; López-Moreno, Juan Ignacio; Rahman, Kazi; Beniston, Martin

# Accepted Manuscript

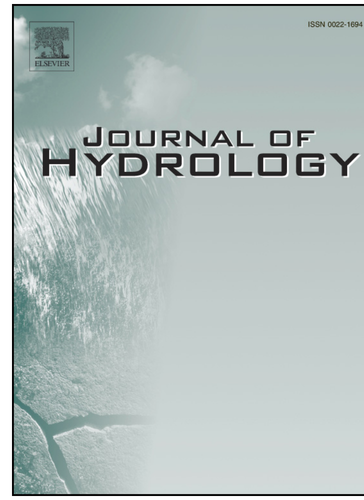


Streamflow timing of mountain rivers in spain: Recent changes and future projections

Enrique Morán-Tejeda, Jorge Lorenzo-Lacruz, Juan Ignacio López-Moreno, Kazi Rahman, Martin Beniston

PII: S0022-1694(14)00513-7
DOI: http://dx.doi.org/10.1016/j.jhydrol.2014.06.053
Reference: HYDROL 19727

To appear in: *Journal of Hydrology*

Received Date: 12 February 2014
Revised Date: 20 May 2014
Accepted Date: 28 June 2014

Please cite this article as: Morán-Tejeda, E., Lorenzo-Lacruz, J., López-Moreno, J.I., Rahman, K., Beniston, M., Streamflow timing of mountain rivers in spain: Recent changes and future projections, *Journal of Hydrology* (2014), doi: http://dx.doi.org/10.1016/j.jhydrol.2014.06.053

# STREAMFLOW TIMING OF MOUNTAIN RIVERS IN SPAIN: RECENT CHANGES AND FUTURE PROJECTIONS

Enrique Morán-Tejeda[1,3], Jorge Lorenzo-Lacruz[2], Juan Ignacio López-Moreno[3], Kazi Rahman[4] and Martin Beniston[1]

1. Institute for Environmental Studies, University of Geneva, Switzerland
2. Department of Geography, University of Zaragoza, Spain
3. Pyrenean Institute of Ecology, CSIC, Spain
4. School of Earth Sciences, Stanford University, USA

Corresponding author: Enrique Morán-Tejeda
e-mail: enriquemoran@gmail.com
phone number: +34 976369393 ext 880033

ABSTRACT

Changes in streamflow timing are studied in 27 mountain rivers in Spain, in the context of climate warming. The studied rivers are characterized by a highflows period in spring due to snowmelt, although differences in the role of snow and consequently in the timing of flows are observed amongst cases. We calculated for every year of the studied period (1976-2008) two hydrological indices that enable locating the timing of spring flows within the annual hydrologic regime, i.e. the day of 75 per cent of mass, and the day of spring maximum. The evolution of these indices was compared with that of seasonal precipitation and temperature, and trends in time were calculated. Results show a general negative trend in the studied indices which indicates that spring peaks due to snowmelt are shifting earlier within the hydrological year. Spring temperatures, which show a significant increasing trend, are the main co-variable responsible for the observed changes in the streamflow timing. In a second set of analyses we performed hydrological simulations with the SWAT model, in order to estimate changes in streamflow timing under projected warming temperatures. Projections show further shifting of spring peak flows along with a more pronounced low water level period in the summer. The simulations also allowed quantifying the role of snowfall-snowmelt on the observed changes in streamflow.

KEYWORDS: Iberian mountains; Streamflow timing; Peak flows; Snowmelt; Climate warming

## INTRODUCTION

The streamflow pulses of mountain rivers are strongly dependent on the seasonal cycles of temperature, and normally experience a “dormant” stage during the cold season, and rapidly change to an active high-flow stage in spring when the period of snowmelt begins. The pace and magnitude of these stages will depend on the geographic characteristics of the mountains that control temperature regimes; these include elevation, latitude, distance to sea, or exposition to predominant winds.  From a scientific point of view mountain rivers represent a valuable laboratory as they reflect the natural conditions of mountain environments before any disturbance by humans is taking place. River flows are sensitive to many changes occurring in the environment, including changes in climate variables (Arnell 1999), changes in land use and land cover (Foley et al. 2005, López-Moreno et al. 2011), or changes in soil properties (Bormann et al. 2007). The magnitude and timing of flows, or even the physical-chemical properties of water, can directly reflect such changes in the environment. Mountains and the process of snow accumulation-melting are hotspots for climate change impacts (Beniston 2003), due to the high sensitivity of the snow cover to seasonal temperatures, especially in low-to-middle elevation sites (Morán-Tejeda et al. 2013b). Increasing temperatures affect the consolidation of the snowpack in a double manner. Regardless of the precipitation regime, in warm winters the amount of snowfall is reduced as the zero degree isotherm is reached less often, thus there is less accumulation of snow. On the other hand, increasing temperatures in spring will anticipate the melting onset, thus reducing the duration of the snowpack. Reduced snow accumulation and the shortening of the snowpack season have been reported in the main mountain chains at mid latitudes during the last decades, coinciding with the recent global warming (Marty 2008, McCabe and Wolock 2009, Beniston 2012). The consequences of reduced snow accumulation in mountains are broad, including alteration of mountain ecosystems, economic losses in winter-tourism areas, or changes in the hydrological rhythm of mountainous rivers (Barnett et al. 2005, Mellander et al. 2007, Uhlmann et al. 2009).

The hydrological consequences of climate warming and reduced snowpack have been broadly studied in the mountains of North America (Hodgkins et al. 2003, Stewart et al. 2005, Hamlet and Lettenmaier 2007, Kalra et al. 2008) thanks to the extensive monitoring systems on climate variables, snow, and river discharges existing since the beginning or middle of the 20th century. The observations conclude that during the last five decades spring flows resulting from snowmelt are occurring earlier in the season, runoff in the cold season is increasing and consequently runoff in the warm season is decreasing. In European mountains, research has been more scattered spatially, but different studies at smaller scales reached similar conclusions for the Alps (Birsan et al. 2005), and the Pyrenees (López-Moreno and García-Ruiz 2004). Thanks to modeling, Adam et al. (2009) were able to identify the most vulnerable areas in the world in terms of changes on streamflow timing due to increasing temperature.

The headwaters of the main Spanish rivers are located in mountainous territories where late-autumn and winter precipitation falls in the form of snow leading to the formation of a sustained snowpack. In a country historically bound to water scarcity such as Spain, mountain rivers constitute a key element for water and risk management (García-Ruiz et al. 2011). Evidence of this is the large number of reservoirs located in the headwaters of rivers (Batalla et al. 2004, Lopez-Moreno et al. 2009, Morán-Tejeda et al. 2012b), or the water transfers between watersheds that exist or are planned in the Spanish territory. The management patterns of these hydraulic infrastructures are strongly dependent on the seasonal pulses of streamflow, as spring peakflows normally occur at the start of the irrigation season. They are, however, subject to be changed if any shift in the streamflow timing is to occur (López-Moreno et al. 2004).

In this work we analyze the changes in the timing of mountain river flows in the Iberian Peninsula in the context of global warming impacts on snow and water resources. For an observational period (1976-2008) we calculated two hydrological indices that allow locating the timing of spring flows within the annual hydrologic regime, and analyzed their trends and changes in time on a set of rivers characterized by analyzing spring high flows from snow melt. Trends in seasonal temperatures and precipitation were also calculated and considered as possible co-variables for explaining changes in river flows. Moreover we project future changes in flow regimes under climate change scenarios by modeling two catchments with SWAT hydrological model. This enabled quantifying the role of snowpack decline on the projected changes, and predicting spatial differences due to geographic factors.

## 2. DATA AND METHODS

### 2.1 Streamflow and temperature data

Daily streamflow data was collected from the national water agency of Spain, Centro de Estudios Hidrográficos (CEDEX, http://hercules.cedex.es/anuarioaforos/default.asp). To make sure that snowmelt pulses were present in all river regimes, we selected only rivers located in the foothills of mountain systems whose drainage watersheds had a mean elevation exceeding 800 m.a.s.l., and had no presence of reservoirs or impoundment systems upstream of the gauge station. A tradeoff between the maximum number of streamflow series, and the longest period possible was necessary, and thus we selected the data period 1976-2008. Series with inhomogeneities were removed, and filling-in of missing data was only performed in those series with less than 5% of missing daily records. For this we fitted linear regressions between the candidate series (series with missing data) and the reference (neighbor) series. We selected the best correlated series (always $R > 0.7$) and used the fitted linear model for calculating the values that would replace the missing data. Finally a total of 27 (out of the initial 71 mountain series) daily streamflow series were used for analyses (Table 1). Most of the selected stations are located in the northern half of the Iberian Peninsula, which is where the majority of mountain systems with sustained winter snowpack are situated. The exception is the Baetic System, for which only one station located in Sierra Nevada was able to be selected. Other stations located in the southern mountains were discarded as they exhibited either strong human interference or very short data series.

Temperature and precipitation data series were also used to be compared with streamflow indices. For this, we used the climatic database Spain02 (see details in Herrera et al. 2012), which comprises daily temperature and precipitation data for 1950-2008 in a 20x20 km grid for the Spanish territory. From this grid, we selected the pixels lying within the studied catchments and calculated the inter-pixels average, having therefore one temperature and one precipitation series for each streamflow series. A validation of the Spain02 database for mountain areas in Spain can be found in Morán-Tejeda et al. (2013a).

2.2. Statistical analyses

From the knowledge of the Spanish climatology, and the different geographical distribution of the selected stations (Figure 1), we assumed that a variety in the shape of river regimes (despite the common feature of a snow-melting peak) was to be found. In order to confirm this, a Principal Components Analysis (PCA) was carried out with the monthly streamflow sums of each hydrological station as input variables. A rotation of axis (Varimax) was also performed for maximizing the sums of variances of the loading factors and thus the differences in the principal components obtained. Three principal components (PC) were obtained, which together explained 97% of the variance of the original variables. Figure 1 (map) shows the spatial distribution of the obtained PCs (given by the maximum loading factors, i.e., maximum correlation between the original variable and the principal components). It also shows the factorial scores of each component, which represent the standard hydrograph of the rivers that belong to each PC, and the average temperatures and precipitation for the climate series of Spain02 with closest location to the hydrological station. The first PC shows a pluvial-nival hydrograph dominated by two peaks in December and April. Rivers with this hydrograph are located in the Cantabrian Range, and the western part of Central System and Pyrenees. The second PC shows a nival-pluvial pattern, with the main peak located in April, and the second one in February, and rivers within this category are located in the eastern part of the Central System and in the Iberian System. If we look at the precipitation regime, it shows also peaks in winter and spring, therefore the spring peak in streamflow in this group of rivers is clearly a combination of waters from snowmelt and from spring precipitation. The third PC shows a pure snowmelt-dominated regime, with a sole peak in May-June, and the rivers are located in the central-eastern Pyrenees and in the Baetic System (Sierra Nevada).

In order to explore the changes in the timing of the snow-melting spring pulses, a number of indices were calculated from the daily streamflow series, following various approaches described in Cayan et al. (2001), Stewart et al. (2005), Burn (2008) and Clow (2010) . Three of the used indices are based on the day of center of mass (D50M), defined as the day of the hydrological year that records the 50% of the total annual streamflow. According to Cayan et al. (2001) and Stewart et al. (2005), it usually represents the time of the year when the spring pulse occurs in snow fed rivers. Given our observed hydrographs (Figure 1), the D50M would not always be representative of the spring peak in most rivers (PC1 and PC2), as they present an earlier peak in winter. Therefore, for ensuring that we pinpoint the water mass of the spring pulse in all the studied rivers, besides the D50M we calculated the D75M and the D90M, which represent the Julian days in which 75% and 90% of annual streamflow occurs, respectively. The latter (D90M) can be considered a measure of how late in the year the runoff persists (Burn, 2008). The fourth hydrological index corresponds to the julian day between March and June in which the maximum flow occurs (Day of spring maximum, DSM). For making sure that the DSM is not an isolated event we made the computations over the daily series smoothed with a 15-day moving average. In this way the DSM would correspond to the day located in the center of the 15-day window with maximum spring flows. A useful index for locating the timing of the spring flows within the hydrograph is the day of beginning of the melting pulse proposed by Cayan et al. (2001). It is calculated as the day in which the cumulative streamflow anomaly (departure from the average) for the year is most negative, which represent the day after which most of the streamflows are above the average of the year. However, this only works for rivers that stay dormant during the winter, and experience a drastic change to active high-flows as a result of snowmelt. Because of this, we only computed this index for rivers of PC3, that present a pure snowmelt regime. An example of the placement of the indices in the hydrograph is provided in Figure 2. Trends in time of the streamflow indices were computed with the prewhitening procedure described in Yue et al. (2002). This approach removes the autocorrelation in series prior to calculating the Mann-Kendall test and the Thiel-Sen estimator for computing the significance and the slopes of the linear trends respectively. Statistics for such tests can be found in Yue et al. (2002).

## 2.3.Modeling future changes driven by climate warming

In order to assess the changes in the streamflow timing that can occur in future decades under ongoing climate change, hydrological runs under climate change scenarios were performed with the Soil Water Assessment Tool (SWAT). We selected two watersheds that represent the two extremes in the role that snow play on stremaflow timing. One catchment (Curueño) is located in the Cantabrian Range and its representative of the pluvial-nival regime (PC1), whereas the second catchment (Ésera) is located in the most elevated sector of the central Pyrenees and it is representative of the pure nival regime (PC3). SWAT is a process-based distributed model that simulates energy, hydrology, soil temperature, mass transport and land management at different levels of watershed (Arnold et al. 1998, Neitsch et al. 2005). Although primarily developed for modeling crops and managed watersheds, SWAT has been continuously updated and successfully applied for modeling hydrological processes in high mountainous watersheds, including snow accumulation and melting processes (Fontaine et al. 2002, Rahman et al. 2013). For details about the model's watershed partitioning, hydrological routing or physical equations, we refer to the original documentation (Neitsch et al. 2005). Input data (source) necessary for model building included: digital elevation model, land cover (Spanish National Forest Inventory), soil classes (European Soils Database, Joint Research Centre, http://eusoils.jrc.ec.europa.eu/, (Panagos et al. 2012), daily precipitation and temperature (Spain02 database) and daily streamflow series for model calibration.

Prior to hydrological simulations under climate change scenarios, the model needed to be calibrated by comparing model runs with observations. The most important adjustment in model's default configuration was the division of the watersheds in "elevation bands" (Fontaine et al. 2002) which allowed the model to reproduce the lapse rates of temperature and precipitation (TLAPS and PLAPS in SWAT nomenclature) with elevation and so capturing the snow-accumulation and snow-melting signals on river flows. Calibration of parameters was carried out for the period 1996-2006, and included the automatic adjustment of the model's parameters by performing multiple iterations with the AMALGAM algorithm (Vrugt and Robinson 2007). This comprises a combination of four different algorithms for parameter optimization, and was adapted for SWAT by Rahman et al. (2013). The model's performance was assessed based on two statistical indices, the Nash-Sutcliffe Efficiency (NSE, Nash and Sutcliffe 1970) and the percent bias (PBIAS), which are widely recommended for hydrological modeling evaluation (Moriasi et al. 2007). The values obtained after calibration were: NSE = 0.81 and PBIAS = -5.5 for Curueño river (id 2068); and NSE = 0.75 and PBIAS = -7.3 for Ésera river (id 9013), which lay within the ranges of *good* to *very good calibration* (Moriasi et al. 2007). The goodness of fit was as well assessed for an independent set of data (time period), with no further adjustment of parameters. The validation period was 1990-1996, and the values of the two statistics for each case were: NSE = 0.76 and PBIAS = 7.6 for Curueño; NSE = 0.38 and PBIAS = 16.8 for Ésera, which indicate a worse performance of the Ésera model. Despite this lower value of NSE for Ésera, we can observe in Figure 3 that the seasonal dynamics of the flows are well captured for the model in both rivers, thus it is considered suitable for performing runs under climate change scenarios.

The climate change scenarios were created for the 2050 time horizon. For this, we used the changes projected by Regional Climate Models (RCMs) of the ENSEMBLES project database (http://www.ensembles-eu.org/ (Hewitt 2004) for the period 2035-2065 with respect to 1970-2000. These projections are based on the A1B scenario of moderate greenhouse gases emissions (IPCC 2001). From the 14 RCMs used (see Table 2), we calculated the changes in seasonal temperature (deltas) between the two periods for the 25x25 km pixels that lay within the two studied watersheds. We then calculated the multimodel deltas' 10$^{th}$ percentile, average and 90$^{th}$ percentile for obtaining a range of long-term plausible variations in seasonal temperature (Table 2). These deltas were then applied on a daily basis to our observed temperature series, and these "climate change series" were used as inputs for the hydrological runs in the SWAT model. In this way we made sure to provide plausible climate warming, preventing our analyses to be influenced by any bias that the RCMs may present.

# 3. RESULTS

## 3.1. Observed changes in streamflow timing.

Figure 4 shows the 3D representation of daily streamflows during the 1976-2008 period (for representation purposes, a 7-year moving average was applied) in three mountain rivers representative of the three types of hydrograph found with the PCA procedures. The first one corresponds to Tormes river (id 2006, Table 1), which shows a loading factor (correlation) with PC1 = 0.89. The second one illustrates Riaza river (id 2009), with a loading factor with

PC2 = 0.77. The third one represents Ésera river (id 9013), and presents a loading factor with PC3 = 0.95. In the three examples it is noticeable that the spring peak is shifting earlier in time. This is particularly clear in the purest snow-fed river (id 9013), but also in the other rivers, where the inter-annual variability in the shape of the hydrograph is larger. Moreover, in the river representative of PC2 (id 2009), we observe that the spring peak has almost disappeared in recent years, whereas back in the 1970's and 1980's, it was the principal peak of the hydrograph. In order to quantify the magnitude of change in the timing of the spring flows, five hydrological indices were developed and their trends were calculated over time. Table 1 shows the change on time of each index (days per year) according to the Theil-Sen's slope estimator. In general negative slope values are reported for most cases and indices, and the average trend is as well negative. However, in many of the studied rivers the trends were not statistically significant according to the Mann-Kendall test, especially for D50M and D90M. Of the studied indices, those that present less variability in trend values amongst cases, and thus a more homogenous evolution are D75M and DSM (SPD presents even lower standard deviation, but it only accounts for four cases, thus is not representative enough). In the following sections we focus our analyses on D75M and DSM as they appear to be the most representative indices for characterizing spring flows in our rivers sample.

Figure 5a shows the regional evolution of the two indices (average and interquartile range of all stations). A negative trend can be seen in both indices, although DSM shows larger variability at both, temporal and spatial (amplitude of the interquartile range) basis. The average trend of D75M and DSM shows a decrease of nearly 0.5 days per year (Table 1). In Figure 5b the trends for each station are shown. A prevalence of negative trends in both D75M and DSM is observed, with many stations experiencing shifting in the spring peak of more than 10 days per decade (i.e. more than one month during the studied period). However, according to the Mann-Kendall test only 10 and 8 of these trends are significant at a 95% level of confidence for the D75M and DSM respectively. In Figure 6, the magnitudes of observed trends are classified by PCs and by mean elevation of the watersheds in order to find any pattern in the distribution of trends. Considering the principal components, it is seen that rivers of PC3 generally experienced the greatest negative trends in hydrological indices, and rivers of PC2 showed the weakest trends. Elevation-wise there are no clear patterns, which indicates that elevation is not a factor that affects the trends in streamflow timing.

The main hypothesis of this work is that any shift towards earlier spring flows must be associated with a decrease in the snowfall/precipitation ratio, as well as an earlier onset of snowmelt; both processes are closely linked with increasing temperatures. Figure 7 shows the trends that seasonal (winter and spring) and annual temperatures have experienced during the studied period. Winter temperatures do not show homogeneous trends, with positive and negative coefficients indistinctly scattered across the territory. On the contrary, spring temperatures did experience negative and significant trends in most series analyzed, with many of them showing a warming of more than 1ºC per decade. Annual temperatures show, in most cases, negative trends with long-term changes ranging between 0.25 and 1.0ºC per decade. In Figure 8 we show the correlations between hydrological indices and seasonal temperature. For every station we found that a seasonal temperature aggregate (winter, spring, winter-spring, or annual) correlated better with the hydrological index. Figure 8.a shows an example of one station in which D75M shows a negative (significant) correlation with the mean annual temperature (Tm annual), and DSM shows a negative (significant) correlation with mean spring temperature. Figure 8b shows the correlation for all stations. D75M shows negative correlations with temperature in all stations, and these are significant (at 95% of confidence level) in the majority of cases. The temperature aggregate that better correlates with D75M is the Tm annual in 15 cases, Tm spring in 6, Tm winter-spring in 6, and Tm winter in one case. On the contrary, DSM only correlates significantly with temperature in 5 stations.

Trends in precipitation may play an important role in the shifts of peak flows as well, especially in those rivers with a bi-modal (rainfall-snow) regime. We saw how precipitation peaks in both winter and spring, thus coinciding in the majority of cases (except in PC3 rivers) with the peak flows. Thus, any trend in winter and spring precipitation could be responsible for the observed changes in peak flows. To verify this, we undertook the same analyses as for temperature (seasonal trends and correlation with hydrological indices) with the precipitation series. A summary of the results is presented in Table 3. Regarding trends, we observe that in winter, a majority of coefficients were negative (24 negative versus 3 positive), but there is only one statistically significant trend. Spring and annual precipitation show in contrast predominance of positive coefficients, but only two cases (one negative and one positive) can be designed as significant trends. Regarding the correlation of seasonal precipitation with hydrological indices, we observe no clear pattern, and very few statistically significant correlations. Winter precipitation shows 8 positive correlations (zero significant) and 19 negative (only 3 significant) with D75M, whereas it shows the opposite pattern with DSM: 18 positive (2 significant) and 9 negative (zero significant). Spring precipitation only shows significant positive correlation in 3 cases, for D75M and non-significant correlations with DSM. Finally, annual precipitation shows one case of positive significant correlation with D75M and one with DSM, and three cases of negative significant correlation with D75M. It must be highlighted that the few significant correlations found (data not shown) were always R less than 0.5. These results indicate that precipitation may partially explain the trends observed in the hydrological indices but only in few cases, and potentially enhancing the effect of increasing temperatures.

## 3.2. Projected changes in streamflow timing by climate warming

Hydrological runs under a projected warmer climate for two of the studied rivers were performed applying the deltas in seasonal temperature to the SWAT model inputs depicted in Table 2 (see 2.3 section for full explanation). In section 2.3 we demonstrated that the model is able to reproduce the seasonal dynamics of observed river flows after performing calibration. Figure 9 shows that the model is also capturing the trends and variability of the observed timing indices in the two modeled watersheds: Curueño (Figure 9a) Ésera (Figure 9b). As previously observed in the calibration section (Fig. 3), the variability is slightly worse captured for Ésera than for Curueño. The trends are, however, well simulated, which indicates that the model is capturing the signal of the increasing temperatures on the timing of streamflows.

Figure 10 shows the changes in streamflow timing projected for the same rivers under the climate change scenarios. As SWAT allows the simulation of the quantity of water contained in the snowpack (expressed as Snow Water Equivalent, SWE) on a daily basis, we also show changes in this parameter, given its importance on controlling streamflow seasonality. For the Curueño river (Figure 9a) we observe that streamflows in March-to-May decrease when temperatures increase, and that flows increase in December-January, indicating a change in the rainfall/snowfall ratio. The bar plot shows the change in annual streamflow as well, indicating small drops in water volume (between 3% and 4%), which are associated with increasing evapotranspiration under warmer conditions. In the right plot we observe the snow water content and its irregular behavior during the snow season with many fluctuations and two main peaks around early February and early March (125th and 160th Julian days). When considering climate change scenarios it experiences a large drop as well as shifting peaks. For the 10th percentile of multimodel warming already a 49% decrease in SWE is observed; then it drops to 61% and 69% for the average and the 90th percentile deltas respectively. For the Ésera river (Figure 10b) the magnitude and duration of streamflow changes are larger than in the previous example. The decrease in spring streamflows under climate change scenarios starts later (May), but lasts until the end of the hydrological year (September). Consequently, streamflow experience increases from early winter to early spring, therefore giving a much more altered river regime than for the Curueño river. Even so, the shape of the hydrograph remains similar, with spring still exhibiting the principal peak of the hydrological year. The net change in annual discharge is negligible (less than 3%) and it is related to the effect of evapotranspiration on the annual water balance. We observe that the snowpack behavior, in both current and future climatic conditions, is different with respect to the Curueño river. In this case, the SWE shows a more regular distribution throughout the snow season, with not so many ups and downs as in the previous case, and it peaks later in time (between early March and late April). Under warmer conditions, the decrease in the amount of SWE is evident and the peak of April has practically disappeared. In relative terms, the loss of snow is not as large as in the Curueño watershed (from 33% to 56%), indicating a larger resistance of the snowpack to atmospheric warming. Even if the loss of SWE is smaller, we also observe that streamflow changes are larger in this case, thus implying that snow is a much more important component of the water balance and the seasonality of streamflows in rivers of the PC3 category than then rest of studied rivers.

In Table 4a we show the changes in the two hydrological indices (D75M and DSM) for the climate change scenarios compared to current conditions. For the Curueño river, projected changes in D75M are relatively small (3, 4 and 5 days for the different climate change scenarios) compared to changes in DSM (1, 10 and 11 days). The opposite is observed for the Ésera river, with larger changes in D75M (9, 13 and 16 days) compared to DSM (2, 6 and 6 days). This is another indication of the different behavior of the two selected rivers with a contrasting role of snow on the functioning of the hydrological system. The simulated changes in both indices for the future seem to be of smaller magnitude than those observed for 1976-2008 period, and can be attributed to the role of precipitation. In our climate change simulations we did not consider any change in precipitation, and we observed in the previous section that precipitation actually plays only a secondary role in the trends observed in D75M and DSM. In Table 4b we observe as well the ratios snowfall/rainfall and snowmelt/streamflow, and see how they decrease as temperatures increase.

## 4. DISCUSSION AND CONCLUSIONS

We present the first comprehensive study of changes in streamflow timing in mountainous rivers in Spain. Previous studies contemplated the characteristics of river regimes in different watersheds of the Spanish territory. López-Moreno and García-Ruiz (2004) showed the importance of snow-accumulation and melting in watersheds of Central Pyrenees. Morán-Tejeda et al. (2011, 2012a) analyzed the different types of river regimes in the Duero basin, and the causes of changes in the magnitude and timing of streamflows, which included precipitation and temperature trends, land-use changes in the headwaters, and management of reservoirs in downstream areas. Lorenzo-Lacruz et al. (2012) used a large database of Spanish rivers to show trends in monthly streamflow and observed a generalized decrease of winter and spring flows during the last five decades, of differing magnitude depending on the geographical location. In this work, we focused only on mountain rivers not disrupted by major human interference (e.g., dams or reservoirs), to infer the direct influence of observed climate warming on snow-dominated regions. Even though a large number of mountain streamflow series are nowadays available for the Spanish territory, many of them did not present series with a suitable length for a statistical study, while others presented many inconsistencies and data gaps and many of them corresponded to stations located downstream of reservoirs or hydraulic infrastructure. The final number of studied rivers (a total of 27) is, however, representative of the wide variety of mountain rivers in continental Spain, as at least one river in every high-elevation mountain chain was studied. As trends in seasonal river discharges have been already studied in the aforementioned works, we focused here on changes in the timing of streamflow based on daily statistics that gave an idea of how the snow-derived peakflows change on time. In general, the timing indices show negative trends during the studied period, which means that the spring peak derived from snow-melting is either losing relevance with respect to winter flows, or is shifting earlier in time. However, some of the indices present inhomogeneous signal among cases, thus we focused our analysis on those that presented less variability (D75M and DSM). In the majority of cases the observed shift accounts for more than 8 days/decade, i.e. 4 weeks during the studied period. Not all these trends are, however, significant at the 95% confidence level, especially for DSM, which shows greater temporal and spatial variability than D75M. The trend and correlation analyses of climate seasonal aggregates corroborate the hypothesis that increasing temperature (generalized positive trends in spring temperature) in the region is the main factor responsible for the shifting peak flows. Seasonal temperature shows a negative and significant correlation in the majority of cases with the evolution of D75M and, to a lesser extent, with DSM. Precipitation, which also peaks in winter and spring, does not show significant trends over the territory and can only partially explain, in few cases, the evolution of the hydrological indices. Stewart et al. (2005) found as well that increasing spring temperatures was responsible for the earlier springtime flows in large set of snow-dominated rivers in western North America. Hodgkins (2003) also pointed out increasing temperatures as the main cause for changes on streamflow timing in un-altered rivers of New England, USA. Although not looking at changes in streamflow timing, Birsan et al. (2005) hypothesized that observed increases in winter flows in Swiss rivers were related with the increase in temperatures and the consequent shift of snowfall into rainfall. In a global-scale study Adam et al. (2009) demonstrated, through hydrological modeling, that temperatures were the main factor leading to changes in winter and spring flows in snow-dominated regions, regardless of trends in precipitation. A contrasting hydrological trend was observed in highly glaciarized mountains, where increases in summer runoff due to enhanced glacier melting have been reported (Collins 2007, Renard et al. 2008). The decrease in the snowfall/rainfall ratio in winter and the earlier snowmelt in spring are thought to be the main causes for the changes in streamflow timing observed in this work. This is not easy to demonstrate directly, due to the lack of daily snow data that can be compared with climate and hydrological variables. Still, it has been demonstrated that snowpack depth and duration in the mountain ranges of Europe has decreased during the last decades, including the Alps (Scherrer et al. 2004, Marty 2008, Beniston 2012) and the Pyrenees (López-Moreno 2005, Morán-Tejeda et al. 2013a), which is clear evidence of a reduction in the amount of snowfall and increase of temperature

The second objective of this paper was to perform hydrological simulations under projected temperature increase, in order to quantify changes in streamflow timing for the 2050 time horizon. This was done using the SWAT model and only for two of the studied rivers, given the large amount of data and time necessary to build and calibrate the model. We believe, however, that the results obtained for the two simulated watersheds can be extrapolated to the rest of watershed as they reproduce the variety of climatic and geographic characteristics of the studied mountains. The calibrated model was able to reproduce the intra and inter-annual variability, the pluvial and snowmelt peaks, and was therefore suitable to conduct the desired analyses and infer variations in streamflow timing under increased temperatures. The added value of the simulations is that the relative weight of the water balance components can be measured and compared among scenarios. In our case we show the quantity of water in the snowpack (snow water equivalent, SWE) as this is the key factor for understanding changes in streamflow with increasing temperatures. The simulations showed that in the two studied cases SWE experienced a large drop with increasing temperatures, which in turn implies a decrease in the snowfall/rainfall ratio in winter. The hydrological behavior of the two watersheds differs, however, when climate warming is considered. For very similar changes in temperature (see Table 2) the decrease in the amount of snow in the pluvial-snow river (Curueño) is, in relative terms, larger than for the snow-dominated river (Ésera). This can be explained by the differences in elevation between the two watersheds (despite the similar values of average elevation: 1518m and 1528m respectively): in Curueño 50% of the watershed is above 1500m, but only 1% is above 2000m; in contrast, Ésera presents 44% of the watershed above 1500 m, and 28% percent above 2000m. Ésera therefore exhibits a larger area under the zero-degree isotherm and the snowpack will thus be less sensitive to warming than that accumulated at lower elevations, such as in the Curueño watershed. An elevation dependence of the magnitude of changes of snowpack driven by climate change was previously reported by López-Moreno et al. (2009). In spite of this, the changes in streamflow timing are of greater magnitude in the Ésera than in the Curueño Basins, and the cause of this is linked to the different importance of snowmelt as a component of the water balance, which is more important in the former (45%) than in the latter (40%).

It must be stressed that the projected changes in streamflow timing should only be considered as being illustrative and not robust predictions, since many uncertainties related to climate and hydrological modeling are still present. We present a range of possible changes by considering the extremes and average of multimodel temperature deltas. Calibration techniques or the choice of the hydrological model (Beven 2006) can also be important drivers of uncertainty. Moreover, we did not consider in this work any projection of precipitation trends in the future, as we only aimed to assess the isolated role of temperatures on streamflow changes. However any change in the seasonality or in the total amount of precipitation driven by climate warming in the region (Solomon et al. 2007) would imply further changes in the hydrological regime. The majority of projections conclude that precipitation will decrease in future decades in the Iberian Peninsula (Bladé and Castro-Díez 2010), therefore the changes in streamflow reported here are likely to aggravate.

A major problem in the driest areas of Spain is the critical low volume of water in rivers at the end of the hydrological year (late summer), due to climatologic and water demand causes. Many reservoirs were built during the second half of the 20th century to overcome this problem. These are mainly used for irrigation, hydropower and urban supply purposes, and their basic pattern of management includes the storage of water during the highflow season and its release when the water and electricity demand are higher, i.e. during summer. López-Moreno et al. (2004) demonstrated, however, the existence of two different patterns of storage-release of the Yesa reservoir (in central Pyrenees) since it was built, which were used depending on the fluctuations in the hydrological regime. The changes in streamflow timing reported here include both, a displacement of the highflows earlier in the season and a more pronounced low water period in summer, and demonstrate the necessity of flexible schemes of reservoir's management in order to ensure water supply under changing and uncertain availability conditions in the upcoming decades.

## Acknowledgements

This study was possible thanks to financial support from the Spanish Government (Ministry of Education) through the postdoctoral program "Ayudas de movilidad postdoctoral en centros extranjeros (Orden EDU/2728 /2011, de 29 de Septiembre)". It has been as well supported by the research projects: "Hidrología nival en el Pirineo Central Español: Variabilidad espacial, importancia hidrológica y respuesta a la variabilidad y cambio climático (CGL2011-27536/HID, Hidronieve)", financed by the Spanish Commission of Science and Technology and FEDER; and CTTP1/12 "Creación de un modelo de alta resolución espacial para cuantificar la esquiabilidad y la afluencia turística en el Pirineo bajo distintos escenarios de cambio climático", financed by the Comunidad de Trabajo de los Pirineos. We acknowledge the two anonymous reviewers for the constructive comments that helped improving the final version of the manuscript

## REFERENCES

Adam, J. C., A. F. Hamlet, and D. P. Lettenmaier. 2009. Implications of global climate change for snowmelt hydrology in the twenty-first century. Hydrological Processes **23**:962-972.

Arnell, N. W. 1999. The effect of climate change on hydrological regimes in Europe: a continental perspective. Global Environmental Change-Human and Policy Dimensions **9**:5-23.

Arnold, J. G., R. Srinivasan, R. S. Muttiah, and J. R. Williams. 1998. Large area hydrologic modeling and assessment part I: Model development1. JAWRA Journal of the American Water Resources Association **34**:73-89.

Barnett, T. P., J. C. Adam, and D. P. Lettenmaier. 2005. Potential impacts of a warming climate on water availability in snow-dominated regions. Nature **438**:303-309.

Batalla, R. J., C. M. Gómez, and G. M. Kondolf. 2004. Reservoir-induced hydrological changes in the Ebro River basin (NE Spain). Journal of Hydrology **290**:117-136.

Beniston, M. 2003. Climatic Change in Mountain Regions: A Review of Possible Impacts. Climatic Change **59**:5-31.

Beniston, M. 2012. Is snow in the Alps receding or disappearing? WIREs Climate Change (Wiley Interdisciplinary Reviews / Climate Change), doi: 10.1002/wcc.179

Beven, K. 2006. A manifesto for the equifinality thesis. Journal of Hydrology **320**:18-36.

Birsan, M. V., P. Molnar, P. Burlando, and M. Pfaundler. 2005. Streamflow trends in Switzerland. Journal of Hydrology **314**:312-329.

Bladé, I. and Y. Castro-Díez. 2010. Tendencias atmosféricas en la Península Ibérica durante el periodo instrumental en el contexto de la variabilidad natural.*in* F. Pérez and R. Boscolo, editors. Clima en España: pasado, presente y futuro. 25-42 pp.

Bormann, H., L. Breuer, T. Gräff, and J. A. Huisman. 2007. Analysing the effects of soil properties changes associated with land use changes on the simulated water balance: A comparison of three hydrological catchment models for scenario analysis. Ecological modelling **209**:29-40.

Burn, D. H. 2008 Climatic influences on streamflow timing in the headwaters of the Mackenzie River Basin. J. Hydrol. 352 225-238

Cayan, D. R., M. D. Dettinger, S. A. Kammerdiener, J. M. Caprio, and D. H. Peterson. 2001. Changes in the Onset of Spring in the Western United States. Bulletin of the American Meteorological Society **82**:399-415.

Clow, D. W. 2010 Changes in the timing of snowmelt and streamflow in Colorado: A response to recent warming. J. Clim. 23 2293-2306

Collins, D. N. 2007. Changes in quantity and variability of runoff from Alpine basins with climatic fluctuation and glacier decline. IAHS-AISH publication:75-85.

Foley, J. A., R. DeFries, G. P. Asner, C. Barford, G. Bonan, S. R. Carpenter, F. S. Chapin, M. T. Coe, G. C. Daily, H. K. Gibbs, J. H. Helkowski, T. Holloway, E. A. Howard, C. J. Kucharik, C. Monfreda, J. A. Patz, I. C. Prentice, N. Ramankutty, and P. K. Snyder. 2005. Global Consequences of Land Use. Science **309**:570-574.

Fontaine, T., T. Cruickshank, J. Arnold, and R. Hotchkiss. 2002. Development of a snowfall–snowmelt routine for mountainous terrain for the soil water assessment tool (SWAT). Journal of Hydrology **262**:209-223.

García-Ruiz, J. M., J. I. López-Moreno, S. M. Vicente-Serrano, T. Lasanta-Martínez, and S. Beguería. 2011. Mediterranean water resources in a global change scenario. Earth-Science Reviews **105**:121-139.

Hamlet, A. F. and D. P. Lettenmaier. 2007. Effects of 20th century warming and climate variability on flood risk in the western US. Water Resources Research **43**.

Herrera, S., J. M. Gutiérrez, R. Ancell, M. Pons, M. Frías, and J. Fernández. 2012. Development and analysis of a 50-year high-resolution daily gridded precipitation dataset over Spain (Spain02). International Journal of Climatology **32**:74-85.

Hewitt, C. D. 2004. Ensembles-based predictions of climate changes and their impacts. Eos, Transactions American Geophysical Union **85**:566-566.

Hodgkins, G. A., R. W. Dudley, and T. G. Huntington. 2003. Changes in the timing of high river flows in New England over the 20th Century. Journal of Hydrology **278**:244-252.

IPCC. 2001. Climate Change 2001: The scientific bases. Contribution of Working Group I to the Third Assessment Report of the Intergovermental Panel on Climate Change. Houghton, J.T., Ding, Y., Griggs, D.J., Noguer, M., van der Linden, P.J.; Dai, X., Maskell, K. & Johnson, C.A. (eds) Cambridge University Press, United Kingdom. 881 pp.

Kalra, A., T. Piechota, R. Davies, and G. Tootle. 2008. Changes in U.S. Streamflow and Western U.S. Snowpack. Journal of Hydrologic Engineering **13**:156-163.

López-Moreno, J., S. Goyette, and M. Beniston. 2009. Impact of climate change on snowpack in the Pyrenees: Horizontal spatial variability and vertical gradients. Journal of Hydrology **374**:384-396.

López-Moreno, J. I. 2005. Recent variations of snowpack depth in the central Spanish Pyrenees. Arctic Antarctic and Alpine Research **37**:253-260.

López-Moreno, J. I., S. Beguería, and J. M. García-Ruiz. 2004. The management of a large Mediterranean reservoir: Storage regimens of the Yesa Reservoir, Upper Aragon River Basin, central Spanish Pyrenees. Environmental Management **34**:508-515.

López-Moreno, J. I. and J. M. García-Ruiz. 2004. Influence of snow accumulation and snowmelt on streamflow in the central Spanish Pyrenees. Hydrological Sciences Journal-Journal Des Sciences Hydrologiques **49**:787-802.

Lopez-Moreno, J. I., S. M. Vicente-Serrano, S. Begueria, J. M. Garcia-Ruiz, M. M. Portela, and A. B. Almeida. 2009. Dam effects on droughts magnitude and duration in a transboundary basin: The Lower River Tagus, Spain and Portugal. Water Resources Research **45**.

López-Moreno, J. I., S. M. Vicente-Serrano, E. Morán-Tejeda, J. Zabalza, J. Lorenzo-Lacruz, and J. M. García-Ruiz. 2011. Impact of climate evolution and land use changes on water yield in the Ebro basin. Hydrology and Earth System Sciences **15**:311-322.

Lorenzo-Lacruz, J., S. M. Vicente-Serrano, J. I. López-Moreno, E. Morán-Tejeda, and J. Zabalza. 2012. Recent trends in Iberian streamflows (1945–2005). Journal of Hydrology **414–415**:463-475.

Marty, C. 2008. Regime shift of snow days in Switzerland. Geophysical Research Letters **35**.

McCabe, G. J. and D. M. Wolock. 2009. Recent Declines in Western U.S. Snowpack in the Context of Twentieth-Century Climate Variability. Earth Interactions **13**:1-15.

Mellander, P.-E., M. O. Löfvenius, and H. Laudon. 2007. Climate change impact on snow and soil temperature in boreal Scots pine stands. Climatic Change **85**:179-193.

Morán-Tejeda, E., A. Ceballos-Barbancho, J. Llorente-Pinto, and J. López-Moreno. 2012a. Land-cover changes and recent hydrological evolution in the Duero Basin (Spain). Regional Environmental Change **12**:17-33.

Morán-Tejeda, E., S. Herrera, J. Ignacio López-Moreno, J. Revuelto, A. Lehmann, and M. Beniston. 2013a. Evolution and frequency (1970–2007) of combined temperature–precipitation modes in the Spanish mountains and sensitivity of snow cover. Regional Environmental Change **13**:873-885.

Morán-Tejeda, E., J. I. López-Moreno, and M. Beniston. 2013b. The changing roles of temperature and precipitation on snowpack variability in Switzerland as a function of altitude. Geophysical Research Letters **40**:2131-2136.

Morán-Tejeda, E., J. I. López-Moreno, A. Ceballos-Barbancho, and S. M. Vicente-Serrano. 2011. River regimes and recent hydrological changes in the Duero Basin (Spain). Journal of Hydrology.

Morán-Tejeda, E., J. Lorenzo-Lacruz, J. I. López-Moreno, A. Ceballos-Barbancho, J. Zabalza, and S. M. Vicente-Serrano. 2012b. Reservoir Management in the Duero Basin (Spain): Impact on River Regimes and the Response to Environmental Change. Water Resources Management **26**:2125-2146.

Moriasi, D., J. Arnold, M. Van Liew, R. Bingner, R. Harmel, and T. Veith. 2007. Model evaluation guidelines for systematic quantification of accuracy in watershed simulations. Transactions of the Asabe **50**:885-900.

Nash, J. and J. Sutcliffe. 1970. River flow forecasting through conceptual models part I—A discussion of principles. Journal of Hydrology **10**:282-290.

Neitsch, S., J. Arnold, J. Kiniry, J. Williams, and K. King. 2005. Soil and water assessment tool: theoretical documentation, version 2005. Texas, USA.

Panagos, P., M. Van Liedekerke, A. Jones, and L. Montanarella. 2012. European Soil Data Centre: Response to European policy support and public data requirements. Land Use Policy **29**:329-338.

Rahman, K., C. Maringanti, M. Beniston, F. Widmer, K. Abbaspour, and A. Lehmann. 2013. Streamflow Modeling in a Highly Managed Mountainous Glacier Watershed Using SWAT: The Upper Rhone River Watershed Case in Switzerland. Water Resources Management **27**:323-339.

Renard, B., M. Lang, P. Bois, A. Dupeyrat, O. Mestre, H. Niel, E. Sauquet, C. Prudhomme, S. Parey, E. Paquet, L. Neppel, and J. Gailhard. 2008. Regional methods for trend detection: Assessing field significance and regional consistency. Water Resources Research **44**:W08419.

Scherrer, S. C., C. Appenzeller, and M. Laternser. 2004. Trends in Swiss Alpine snow days: The role of local- and large-scale climate variability. Geophysical Research Letters **31**.

Solomon, S., D. Qin, M. Manning, Z. Chen, and M. Marquis. 2007. Climate Change 2007: The Physical Science Basis: Contribution of Working Group I to the Fourth Assessment Report of the Intergovernmental Panel on Climate Change. Cambridge Univ. Press New York.

Stewart, I. T., D. R. Cayan, and M. D. Dettinger. 2005. Changes toward earlier streamflow timing across western North America. Journal of Climate **18**:1136-1155.

Uhlmann, B., S. Goyette, and M. Beniston. 2009. Sensitivity analysis of snow patterns in Swiss ski resorts to shifts in temperature, precipitation and humidity under conditions of climate change. International Journal of Climatology **29**:1048-1055.

Vrugt, J. A. and B. A. Robinson. 2007. Improved evolutionary optimization from genetically adaptive multimethod search. Proceedings of the National Academy of Sciences **104**:708-711.

Yue, S., P. Pilon, B. Phinney, and G. Cavadias. 2002. The influence of autocorrelation on the ability to detect trend in hydrological series. Hydrological Processes **16**:1807-1829.

## Tables

Table 1. Studied rivers and geographic characteristics. PC: principal component; Change on time (days per decade according to Thiel-Sen's slope estimator) is shown for every studied index.* indicates two-sided p-value < 0.05 **SPD was one only calculated for rivers of PC3.

| Station id | river name | PC | elevation (m.a.s.l) | Thiel-Sen's slope estimator | | | | |
|---|---|---|---|---|---|---|---|---|
| | | | | D50M | D75M | D90M | DSM | SPD |
| 1295 | Sella | PC1 | 1004.9 | -0.55 | -0.55* | -0.63* | -0.91* | - |
| 1335 | Nalón | PC1 | 1076.8 | -0.55 | -0.86* | -0.97* | -0.79 | - |
| 1365 | Aller | PC1 | 1088.3 | 0.03 | -0.70* | -0.84* | -1.06* | - |
| 2006 | Tormes | PC1 | 1462.4 | -0.13 | -0.24 | -0.20 | 0.11 | - |
| 2034 | Besande | PC1 | 1567.1 | -0.33 | -0.64* | -0.99* | -0.14 | - |
| 2068 | Curueño | PC1 | 1521.3 | 0.32 | -0.42 | 0.21 | -0.21 | - |
| 2101 | Duero | PC1 | 1429.6 | 0.04 | 0.31 | 1.56* | -0.26 | - |
| 3226 | G.St. María | PC1 | 1323.7 | -0.78* | -0.45 | 0.27 | 0.02 | - |
| 3229 | G. Cuartos | PC1 | 1270.1 | -2.06* | -2.00* | -0.29 | 0.0 | - |
| 9063 | Esca | PC1 | 1071.8 | 0.52 | -0.52 | -0.35 | -0.41 | - |
| 9064 | Salazar | PC1 | 958.3 | 0.6 | -0.51 | -0.35 | -0.76* | - |
| 9066 | Irati | PC1 | 1081.2 | -0.21 | -0.36 | 0.42 | -1.33* | - |
| 9170 | Aragón | PC1 | 1076.2 | -0.11 | -0.60* | -0.54* | -0.65 | - |
| 2009 | Riaza | PC2 | 1628.1 | -0.65 | -0.63* | -0.79* | -0.21 | - |
| 2012 | Duratón | PC2 | 1126.1 | -0.22 | 0.29 | 1.30* | -0.21 | - |
| 2016 | Cega | PC2 | 1280.8 | 0.50 | 0.0 | 3.03* | -0.66 | - |
| 2051 | Moros | PC2 | 1592.3 | 0.23 | -0.37 | -0.58 | -0.25 | - |
| 2057 | Pirón | PC2 | 1179.5 | 0.15 | 0.20 | 0.09 | 0.39 | - |
| 9043 | Linares | PC2 | 1305.3 | -0.43 | -0.78 | -0.20 | -0.51 | - |
| 9044 | Cidacos | PC2 | 1334.6 | -0.67 | -1.14* | -1.00* | -0.56 | - |
| 9050 | Tirón | PC2 | 830 | -0.68 | -0.4 | -0.35 | -0.81 | - |
| 9093 | Oca | PC2 | 843.5 | -0.11 | -0.39 | -0.18 | -0.98 | - |
| 9158 | Tirón | PC2 | 1246.8 | -0.42 | -0.21 | -0.14 | 0.0 | - |
| 5086 | Dilar | PC3 | 2011.4 | -0.18 | -0.14 | -2.96* | -0.33 | -0.31 |
| 9013 | Esera | PC3 | 1525.2 | -0.51 | -0.60* | -0.21 | -1.63* | -0.77* |
| 9018 | Aragón | PC3 | 1570.1 | -0.16 | -0.67* | -0.50 | -1.14* | -0.27 |
| 9040 | Ara | PC3 | 1497.9 | 0.16 | -0.62* | -0.67 | -1.00* | -0.54 |

| | | | | | |
|---|---|---|---|---|---|
| Average | -0.23 | -0.47 | -0.22 | -0.49 | -0.47 |
| Standard deviation | 0.52 | 0.45 | 1.01 | 0.43 | 0.20 |

Table 2. Deltas (changes between average temperature in 1970-2000 and 2035-2065) calculated for 14 Regional Climate Models from ENSEMBLE project. 10th percentile, average, and 90th percentile of multimodel deltas are as well shown. Units are Celsius degrees.

| | Curueño | | | | Ésera | | | |
|---|---|---|---|---|---|---|---|---|
| Climate Model | Winter | Spring | Autumn | Summer | Winter | Spring | Autumn | Summer |
| DMI | 2.0 | 1.8 | 2.5 | 2.0 | 2.0 | 1.6 | 2.4 | 1.9 |
| DMI_ECHAM5 | 1.1 | 1.5 | 2.0 | 2.0 | 1.1 | 1.3 | 1.8 | 1.9 |
| ETHZ | 1.7 | 2.5 | 3.8 | 2.6 | 1.9 | 2.5 | 3.8 | 2.7 |
| HadRM3Q0 | 2.3 | 2.5 | 4.1 | 2.7 | 2.1 | 2.5 | 4.1 | 2.5 |
| HadRM3Q3 | 2.0 | 2.1 | 2.7 | 2.2 | 2.1 | 2.0 | 2.7 | 2.0 |
| HadRM3Q16 | 2.3 | 4.0 | 3.9 | 4.0 | 2.4 | 3.8 | 3.9 | 3.7 |
| ICTP | 1.2 | 1.4 | 2.3 | 1.8 | 1.3 | 1.3 | 2.1 | 1.7 |
| KNMI_ECHAM5-r1 | 1.5 | 2.2 | 3.7 | 2.6 | 1.6 | 2.2 | 2.9 | 2.3 |
| KNMI_ECHAM5-r2 | 1.7 | 1.7 | 3.4 | 2.6 | 1.9 | 1.6 | 2.7 | 2.3 |
| KNMI_ECHAM5-r3 | 1.3 | 1.6 | 3.1 | 2.0 | 1.4 | 1.5 | 2.6 | 2.0 |
| MPI | 1.4 | 1.6 | 3.0 | 2.4 | 1.4 | 1.6 | 2.8 | 2.3 |
| SMHI_BCM | 1.0 | 1.1 | 1.6 | 1.3 | 1.5 | 1.2 | 1.2 | 1.0 |
| SMHI_ECHAM5 | 1.2 | 1.2 | 3.1 | 2.0 | 1.2 | 1.2 | 2.7 | 1.9 |
| SMHI_HadCM3Q3 | 1.8 | 1.4 | 2.6 | 1.9 | 1.9 | 1.5 | 2.8 | 1.9 |
| 10th percentile | 1.1 | 1.2 | 2.1 | 1.9 | 1.2 | 1.2 | 1.9 | 1.8 |
| Average | 1.6 | 1.9 | 3.0 | 2.3 | 1.7 | 1.8 | 2.7 | 2.2 |
| 90th percentile | 2.2 | 2.5 | 3.9 | 2.7 | 2.1 | 2.5 | 3.8 | 2.6 |

Table 3. Trends of precipitation on time, and correlations between seasonal precipitation and hydrological indices. Sig: p-value <0.05.

| Precipitation aggregate | Trends (Mann-Kendall) | | | | Correlations (Pearson R) with hydrological indices D75M | | | | DSM | | | |
|---|---|---|---|---|---|---|---|---|---|---|---|---|
| | positive | sig | negative | sig | positive | sig | negative | sig | positive | sig | negative | sig |
| Winter | 3 | 0 | 24 | 1 | 8 | 0 | 19 | 3 | 18 | 2 | 9 | 0 |
| Spring | 18 | 1 | 9 | 1 | 15 | 3 | 12 | 0 | 11 | 0 | 16 | 0 |
| Annual | 15 | 1 | 12 | 1 | 6 | 1 | 21 | 3 | 18 | 1 | 9 | 0 |

Table 4. Hydrological changes obtained from 30-years SWAT simulations under warming conditions for Curueño and Ésera rivers. a) changes in D75M and DSM (absolute values) b) changes in snowfall/rainfall and snowmelt/streamflow ratios (percentage values)

a)

| | Curueño river | | | | Ésera river | | | |
|---|---|---|---|---|---|---|---|---|
| Index | Current | p10 | average | p90 | Current | p10 | average | p90 |
| D75M | 202 | 199 | 198 | 197 | 275 | 266 | 262 | 259 |
| Change | - | -3 | -4 | -5 | - | -9 | -13 | -16 |
| DSM | 201 | 199 | 191 | 190 | 238 | 236 | 232 | 232 |
| Change | - | -2 | -10 | -11 | - | -2 | -6 | -6 |

b)

| | | | | | | | | |
|---|---|---|---|---|---|---|---|---|
| snowfall/rainfall | 31.46 | 21.25 | 17.01 | 13.59 | 25.37 | 19.21 | 16.79 | 14.77 |
| snowmelt/streamflow | 40.34 | 27.73 | 22.44 | 18.09 | 45.86 | 34.56 | 30.31 | 26.75 |

**Figure Captions**

Figure 1.Iberian Peninsula and location of the studied rivers and mountain systems. Symbols indicate the three principal components identified. 1 (Curueño) and 2 (Ésera) indicate the two watersheds modeled with SWAT for projection purposes. Line plots show the standard stremflows regimen of each principal component, and the average temperature and precipitation for the climate series with closest location to the streamflow stations.

Figure 2. Example of placement of the hydrological indices in a hydrograph representative of PC3 . The hydrograph (a) represent the long-term (1976-2008) average of daily streamflows. b) shows the cumulative river flows and the location of the $50^{th}$, $75^{th}$ and $90^{th}$ percentiles. c) shows the cumulative anomalies of flow (departures from the annual average). The minimum cumulative anomaly indicates the onset of the spring pulse.

Figure 3. Simulated (grey dash line) versus observed (black line) river flows for the calibration and validation periods in Curueño (a) and Ésera rivers (b).

Figure 4. Evolution of streamflows in three rivers representative of the variety of river regimes in the Spanish mountains. For graphic representation, smoothing filters have been applied to X axis (15-days moving average) and Y axis (7-years moving average). Z axis and color scale represent streamflow in $m^3$ $s^{-1}$.

Figure 5 Trends in the streamflow indices for the studied rivers. a) Average evolution of the indices (black line) and interquartile range (gray shade) indicating inter-cases variability. b) Red (blue) indicates negative (positive) trends according to Mann-Kendall test and black dots indicate tow-sided p-value $< 0.05$. The circle size indicates the change in days per decade during the studied period, according to the Thiel-Sen slope estimator.

Figure 6. Magnitude of trends in streamflow indices compared by principal component (upper panels) and elevation range (lower panels).

Figure 7. Trends in seasonal and annual temperatures. Red (blue) indicates positive (negative) trends according to Mann-Kendall test and black dots indicate two-sided p-value $< 0.05$. The circle size indicates the change in ºC per decade during the studied period, according to the Thiel-Sen slope estimator.

Figure 8. Correlations between streamflow indices and seasonal temperature aggregates. a) Example of correlations in a hydrological station (id 9040) between D75M and its best predictor (Tm annual) in the right plot, and between DSM and its best predictor (Tm spring) in the left plot.

Temperature Y axis is inverted for representation purposes. b) Map showing the correlations in all stations. Circle size indicates the magnitude of correlation (R), and black dots indicates p-level < 0.05. Colors indicate which seasonal temperature aggregate (winter, spring, winter-spring, or annual) correlates better with the streamflow indices.

Figure 9. Observed (black line) and simulated (dashed gray line) evolution of D75M and DSM for Curueño (a) and Ésera (b) rivers. Trend values represent the change in time according to the Thiel-Sen slope estimator.

Figure 10. Changes in streamflow and snow water equivalent (SWE) under climate change scenarios (percentile 10, average, and percentile 90 of multimodel deltas) with respect to current climate in Curueño river (a) and Ésera river (b) for a 30-years simulation with SWAT model. Bar plots indicate the total annual (stremaflow) and daily (SWE) change in absolute (bar size) and relative (percent value) terms.

Figure 1



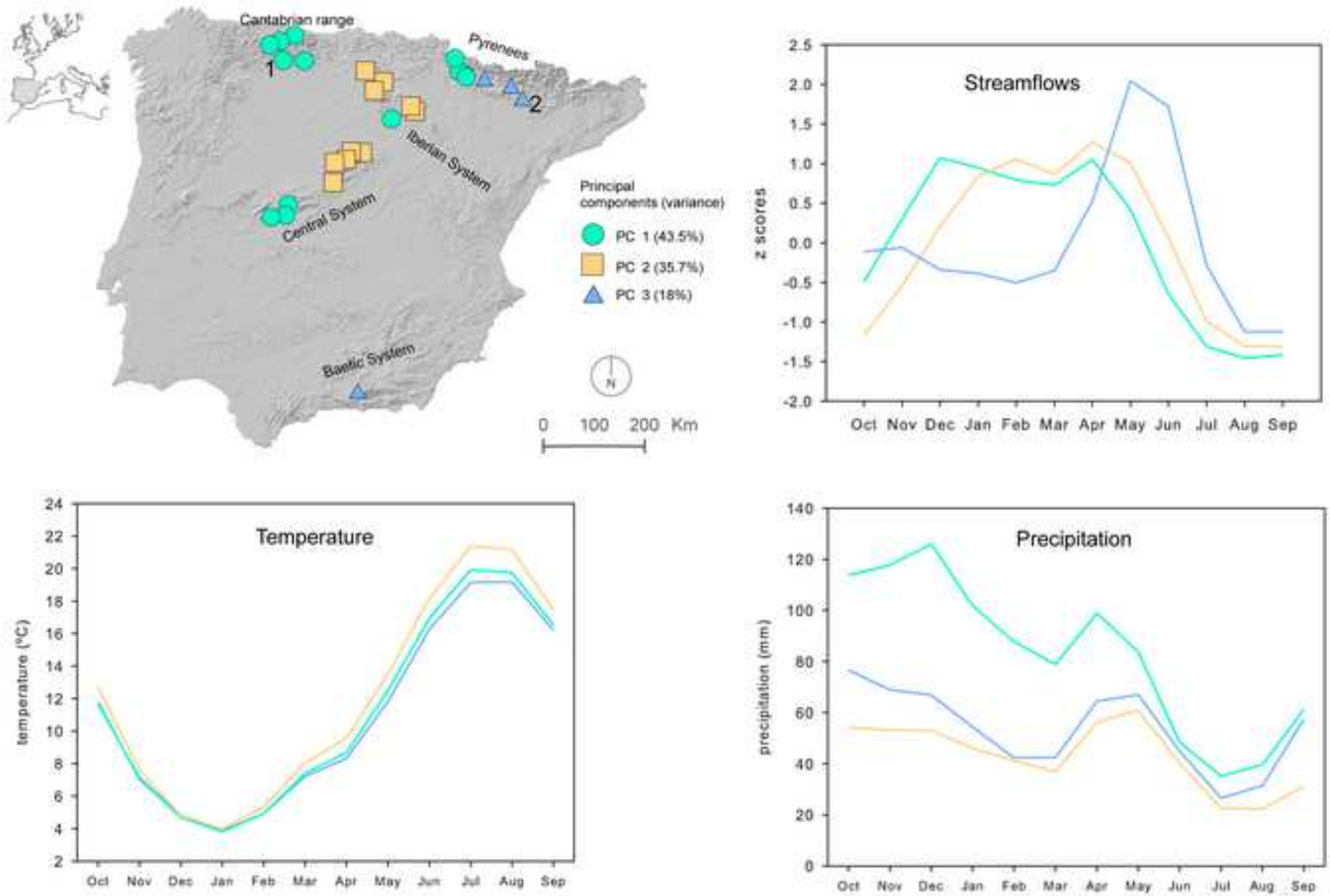
Cantabrian range
Pyrenees
Iberian System
Central System
Baetic System
1
2
Principal components (variance)
PC 1 (43.5%)
PC 2 (35.7%)
PC 3 (18%)
N
0 100 200 Km
Streamflows
z scores
Oct Nov Dec Jan Feb Mar Apr May Jun Jul Aug Sep
Temperature
temperature (ºC)
Precipitation
precipitation (mm)

**Figure 2**



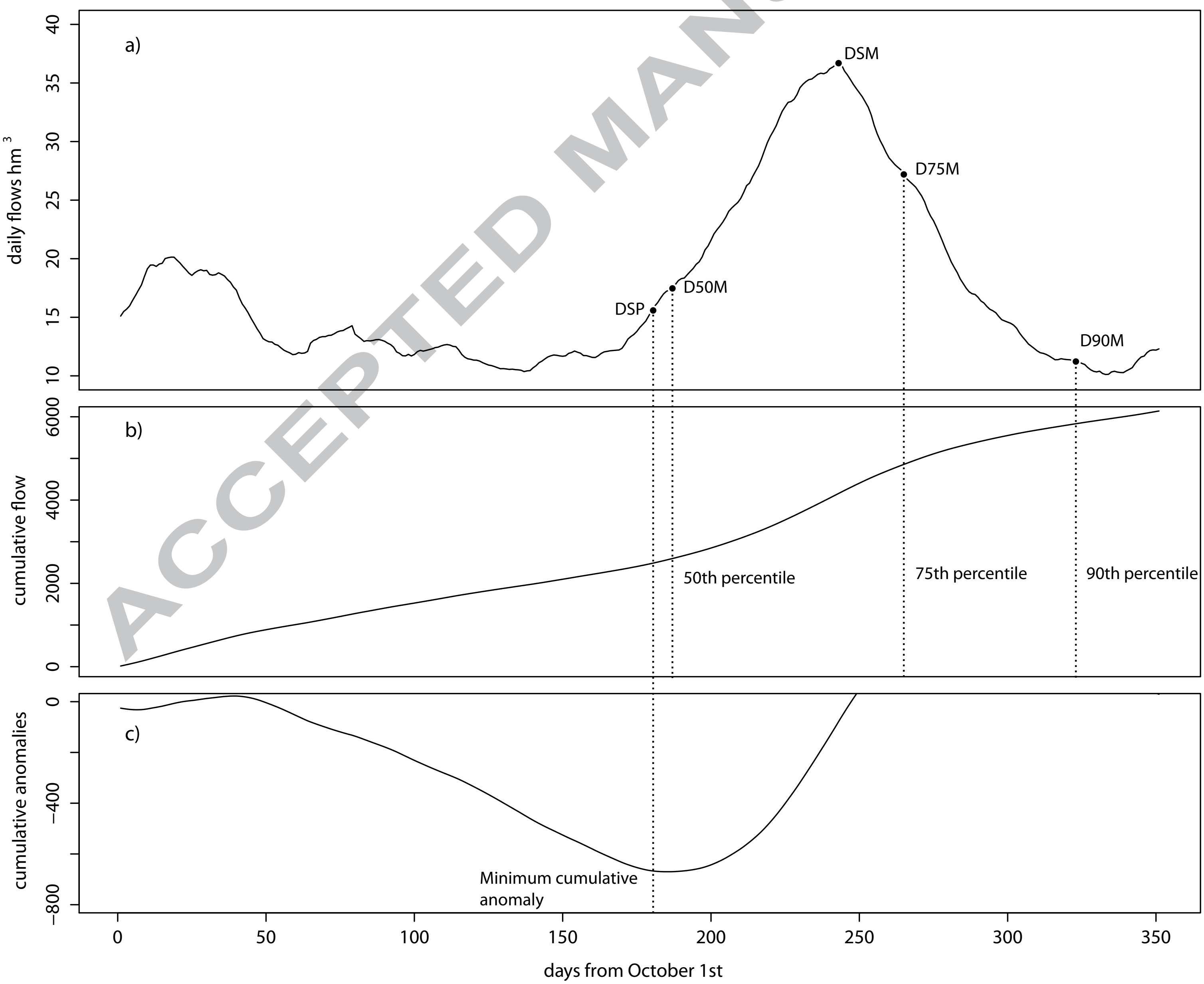
a)
b)
c)
DSM
D75M
D50M
DSP
D90M
50th percentile
75th percentile
90th percentile
Minimum cumulative anomaly
daily flows hm 3
cumulative flow
cumulative anomalies
days from October 1st
10
15
20
25
30
35
40
0
2000
4000
6000
−800
−400
0
50
100
150
200
250
300
350

Figure 3



a)

b)

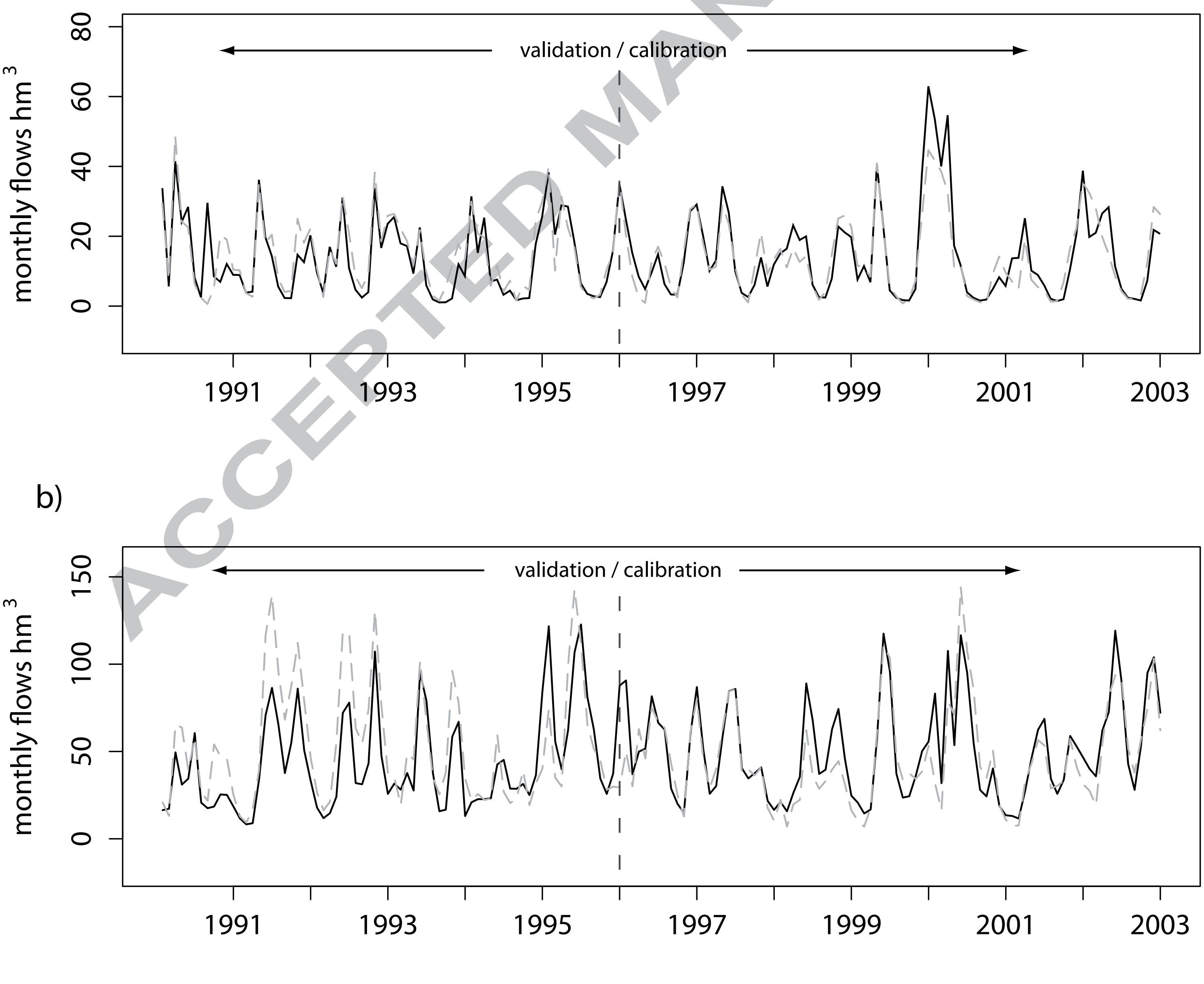

validation / calibration
monthly flows hm 3
0
20
40
60
80
1991
1993
1995
1997
1999
2001
2003
validation / calibration
monthly flows hm 3
0
50
100
150
1991
1993
1995
1997
1999
2001
2003

Figure 4



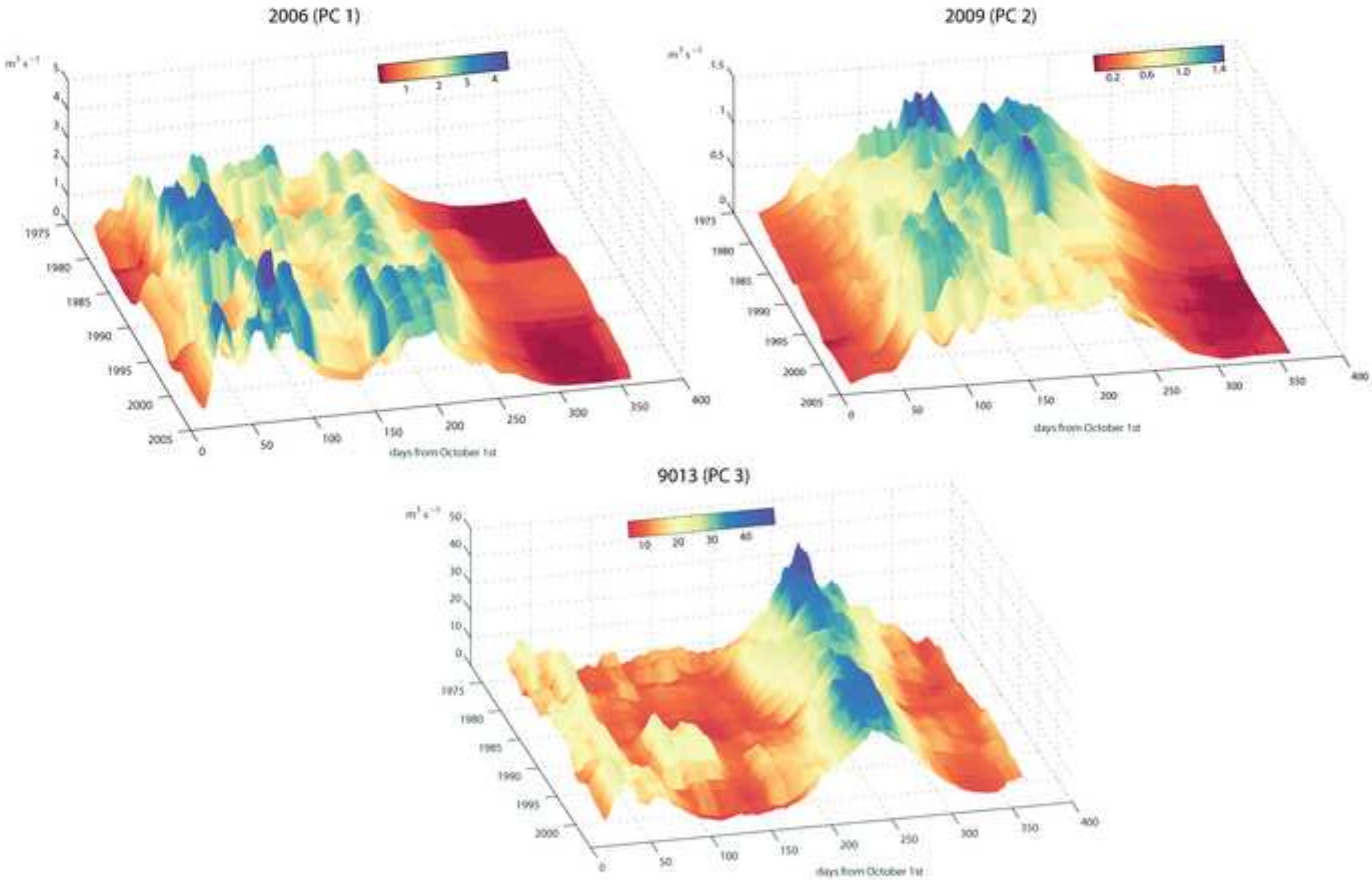
2006 (PC 1)
2009 (PC 2)
9013 (PC 3)
days from October 1st
days from October 1st
days from October 1st
1975
1980
1985
1990
1995
2000
2005
0
50
100
150
200
250
300
350
400

Figure 5



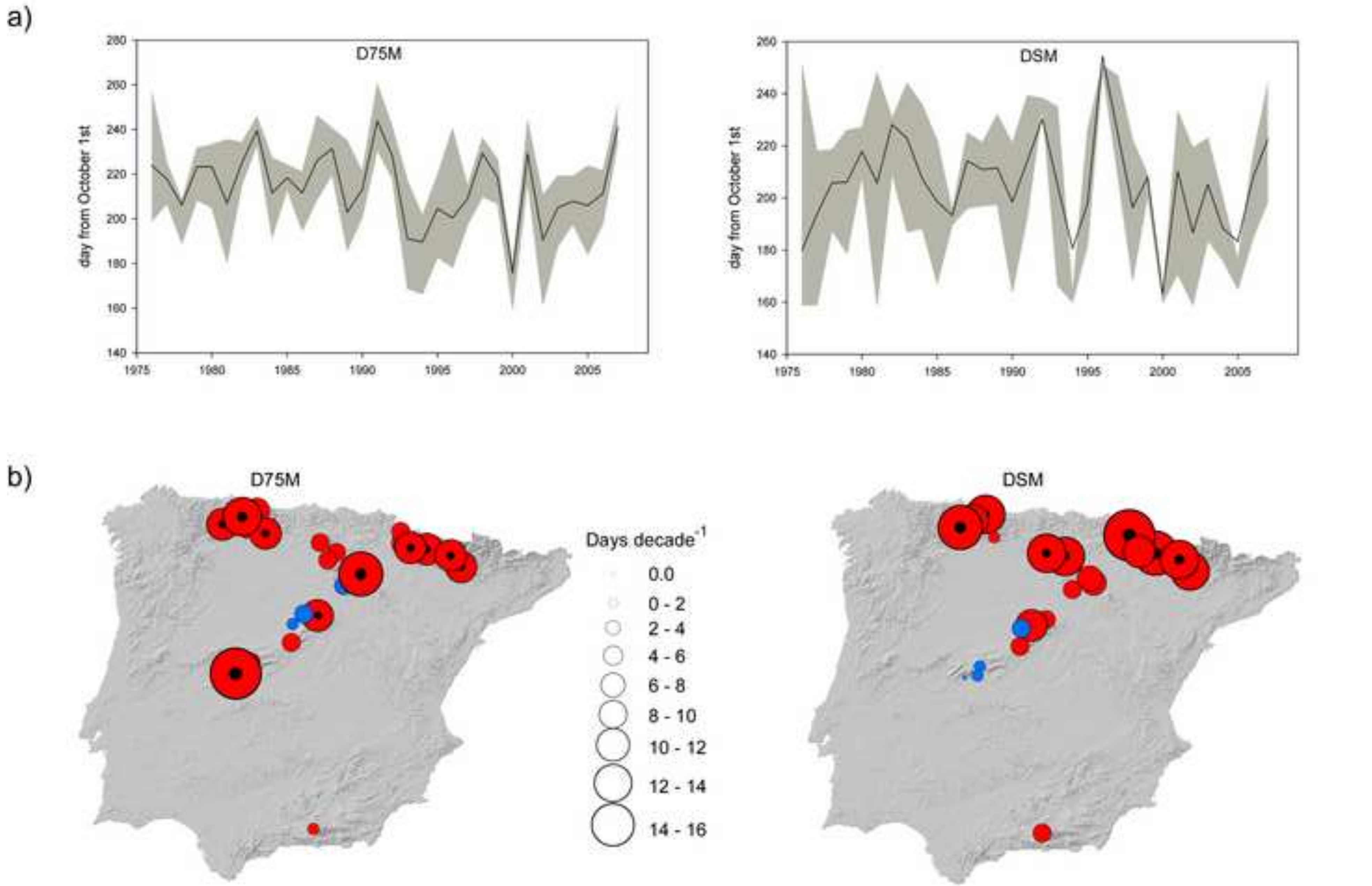
a)
D75M
day from October 1st
280
260
240
220
200
180
160
140
1975
1980
1985
1990
1995
2000
2005
DSM
day from October 1st
260
240
220
200
180
160
140
1975
1980
1985
1990
1995
2000
2005
b)
D75M
DSM
Days decade-1
0.0
0 - 2
2 - 4
4 - 6
6 - 8
8 - 10
10 - 12
12 - 14
14 - 16

Figure 6



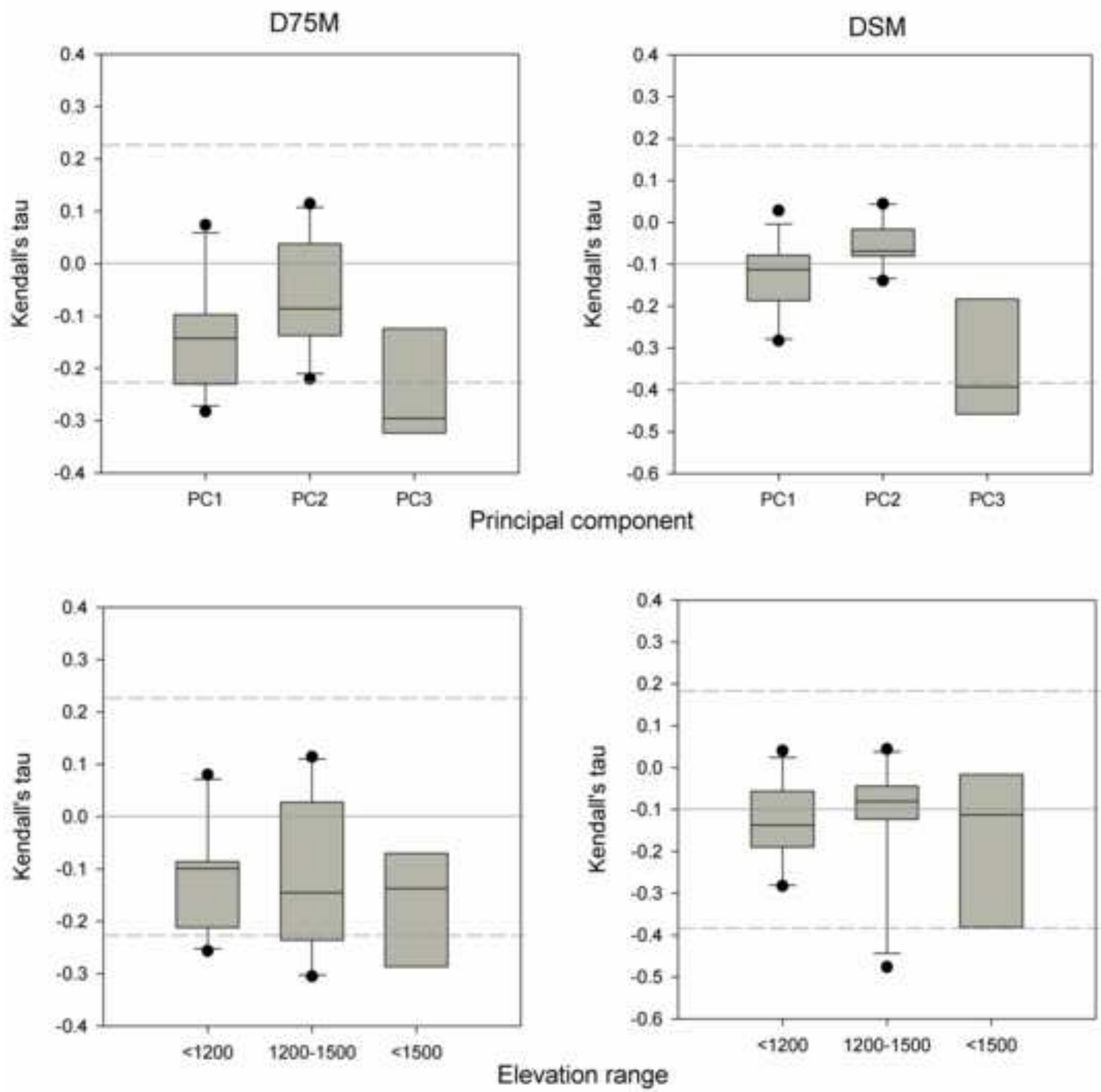
D75M
DSM
0.4
0.3
0.2
0.1
0.0
-0.1
-0.2
-0.3
-0.4
-0.5
-0.6
Kendall's tau
PC1
PC2
PC3
Principal component
<1200
1200-1500
<1500
Elevation range

Figure 7



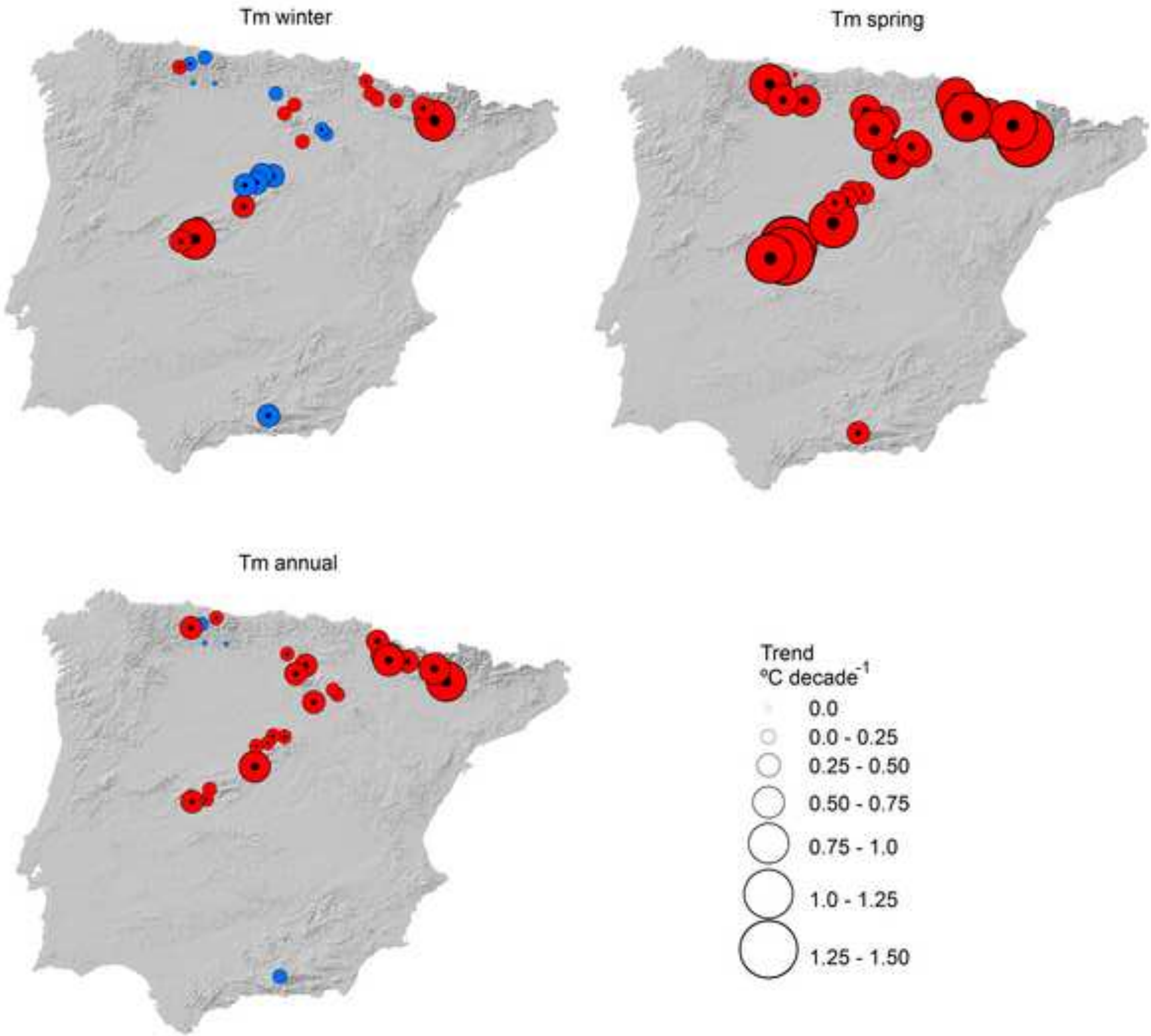
Tm winter
Tm spring
Tm annual
Trend
ºC decade-1
0.0
0.0 - 0.25
0.25 - 0.50
0.50 - 0.75
0.75 - 1.0
1.0 - 1.25
1.25 - 1.50

Figure 8



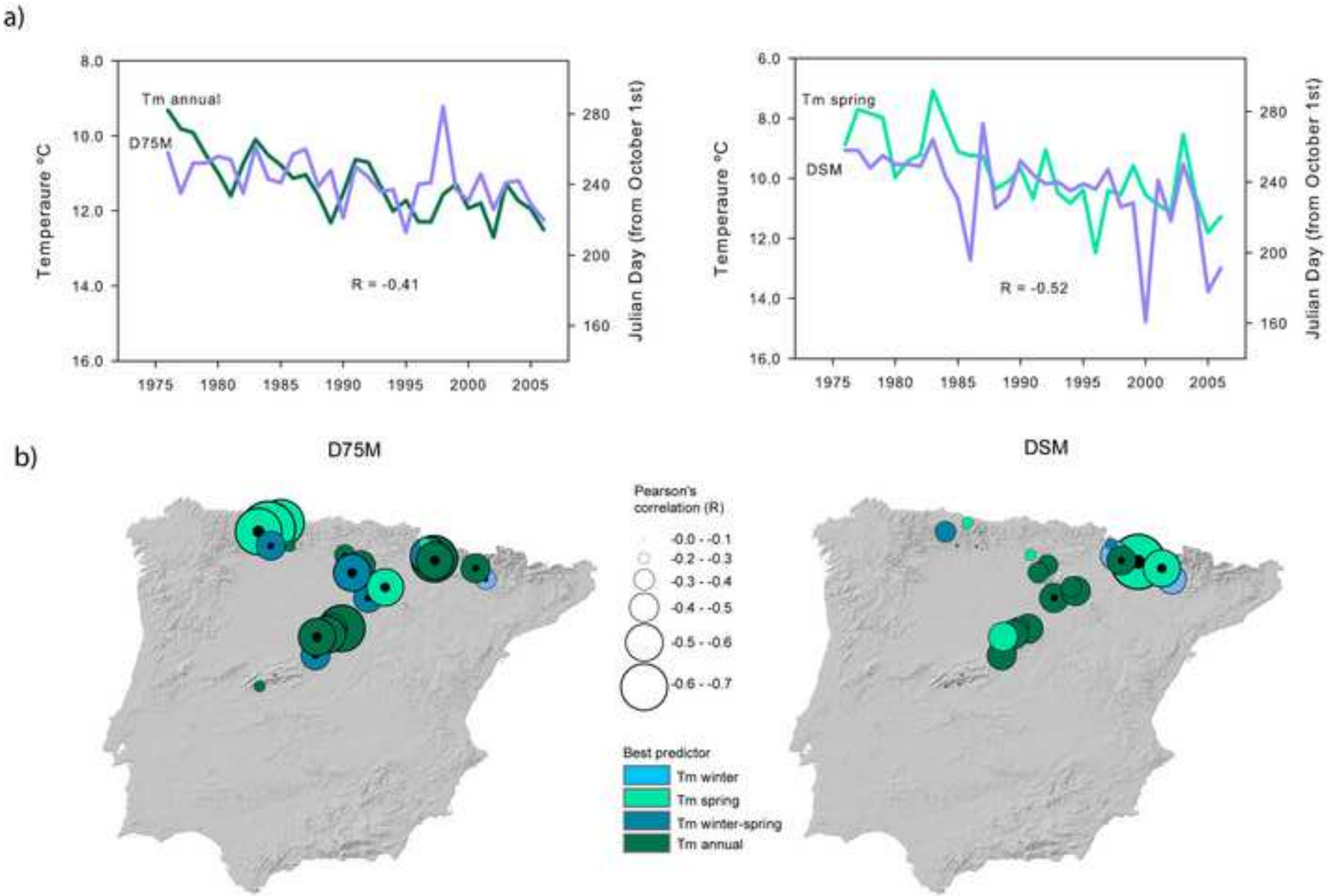
a)
Tm annual
D75M
R = -0.41
Temperaure °C
Julian Day (from October 1st)
Tm spring
DSM
R = -0.52
b)
D75M
DSM
Pearson's correlation (R)
-0.0 - -0.1
-0.2 - -0.3
-0.3 - -0.4
-0.4 - -0.5
-0.5 - -0.6
-0.6 - -0.7
Best predictor
Tm winter
Tm spring
Tm winter-spring
Tm annual

Figure 9



a)

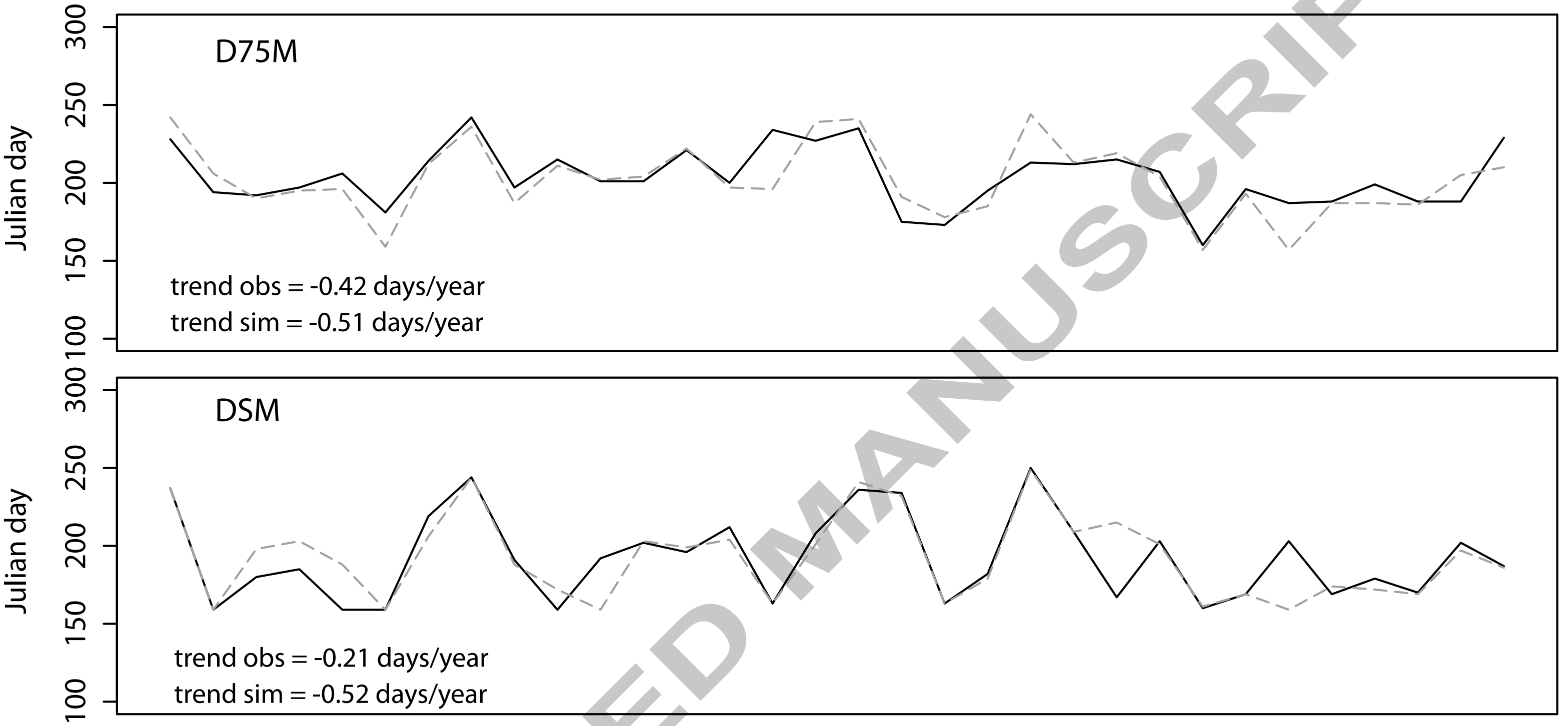
D75M
Julian day
300
250
200
150
100
trend obs = -0.42 days/year
trend sim = -0.51 days/year
DSM
trend obs = -0.21 days/year
trend sim = -0.52 days/year

b)

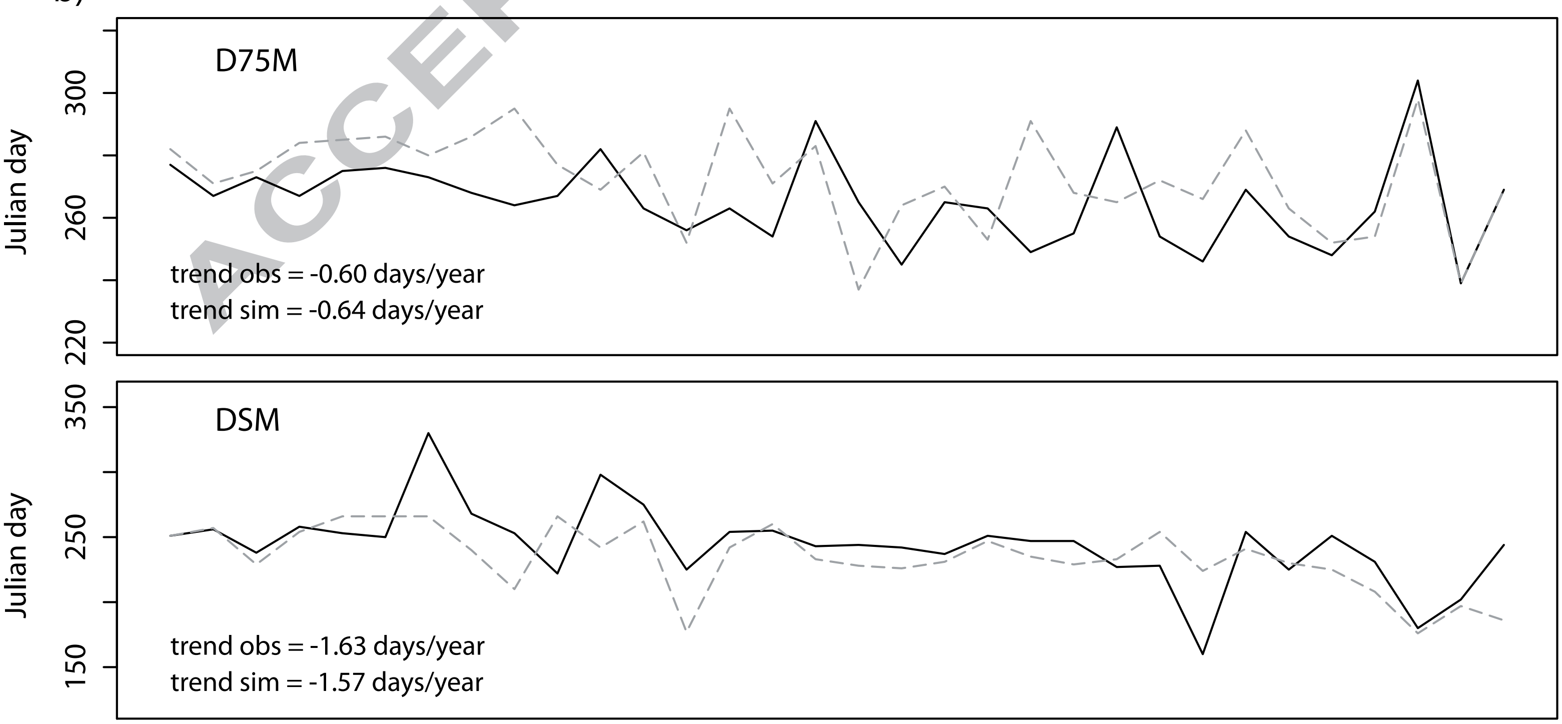
D75M
Julian day
300
260
220
trend obs = -0.60 days/year
trend sim = -0.64 days/year
DSM
350
250
150
trend obs = -1.63 days/year
trend sim = -1.57 days/year

Figure 10



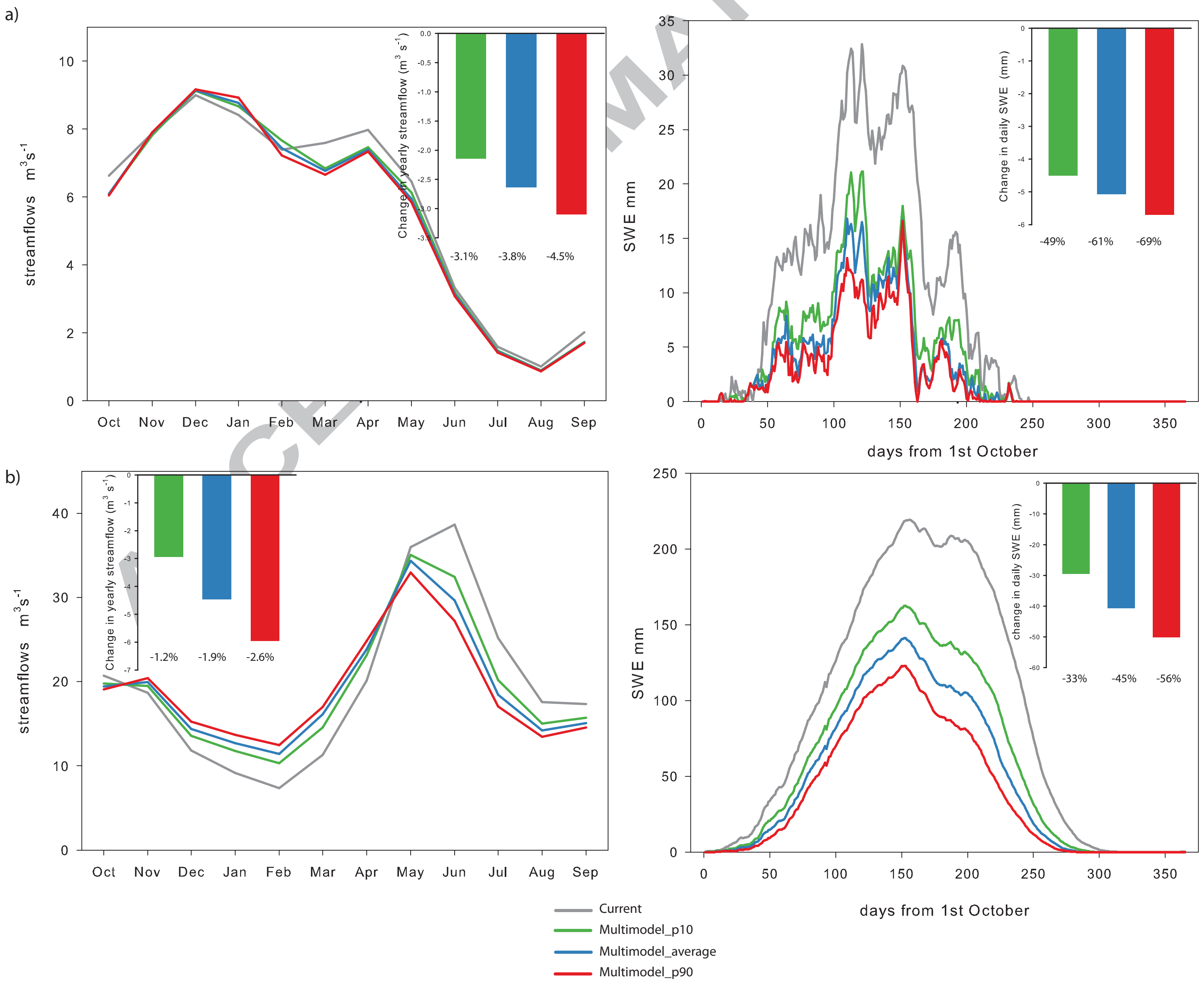

a)
streamflows m$^3$s$^{-1}$
Change in yearly streamflow (m$^3$ s$^{-1}$)
-3.1%
-3.8%
-4.5%
Oct
Nov
Dec
Jan
Feb
Mar
Apr
May
Jun
Jul
Aug
Sep
SWE mm
Change in daily SWE (mm)
-49%
-61%
-69%
days from 1st October
b)
streamflows m$^3$s$^{-1}$
Change in yearly streamflow (m$^3$ s$^{-1}$)
-1.2%
-1.9%
-2.6%
SWE mm
change in daily SWE (mm)
-33%
-45%
-56%
days from 1st October
Current
Multimodel_p10
Multimodel_average
Multimodel_p90

- Spring flows of Spanish mountain rivers moved earlier on time in the last decades
- Increasing temperature is the main climatic variable for explaining such change
- Precipitation showed no trend and little effect on changes on streamflow timing
- Future projections indicate further shift of peak flows derived from snowmelt
- Less snowfall, and faster snowmelt are the underlying processes behind such changes